

Date: 13 Mar 2021
To: "Marcela F. Bolontrade" marcela.bolontrade@hospitalitaliano.org.ar
From: "Patrycja Nowak-Sliwinska" Patrycja.Nowak-Sliwinska@unige.ch
Subject: APPT-D-20-00120R1 - Decision on your Manuscript

Dear Dr. Bolontrade,

We are pleased to inform you that your manuscript has been accepted for publication in Apoptosis. You will receive galley proofs in the near future.

We would like to thank you and your co-authors for submitting this interesting paper to Apoptosis. As the Journal is indexed/abstracted in PubMed, your article will be accessible to readers worldwide.

We look forward to serving you again in the near future.

You will be contacted by Author Services in due course with a link to complete the grant of rights. Please note that you will receive your proofs after the publishing agreement has been received through our system.

Thank you for your contribution to Apoptosis.

Best regards,
Patrycja Nowak-Sliwinska
Editor-in-Chief
Apoptosis

Please note that this journal is a Transformative Journal (TJ). Authors may publish their research through the traditional subscription access route or make their paper open access through payment of an article-processing charge (APC). [Find out more about Transformative Journals](#)

****Our flexible approach during the COVID-19 pandemic****

If you need more time at any stage of the peer-review process, please do let us know. While our systems will continue to remind you of the original timelines, we aim to be as flexible as possible during the current pandemic.

This letter contains confidential information, is for your own use, and should not be forwarded to third parties.

Recipients of this email are registered users within the Editorial Manager database for this journal. We will keep your information on file to use in the process of submitting, evaluating and publishing a manuscript. For more information on how we use your personal details please see our privacy policy at <https://www.springernature.com/production-privacy-policy>. If you no longer wish to receive messages from this journal or you have questions regarding database management, please contact the Publication Office at the link below.

In compliance with data protection regulations, you may request that we remove your personal registration details at any time. (Use the following URL: <https://www.editorialmanager.com/appt/login.asp?a=r>). Please contact the publication office if you have any questions.

Dear Author,

Here are the proofs of your article.

- You can submit your corrections **online**, via **e-mail** or by **fax**.
- For **online** submission please insert your corrections in the online correction form. Always indicate the line number to which the correction refers.
- You can also insert your corrections in the proof PDF and **email** the annotated PDF.
- For fax submission, please ensure that your corrections are clearly legible. Use a fine black pen and write the correction in the margin, not too close to the edge of the page.
- Remember to note the **journal title**, **article number**, and **your name** when sending your response via e-mail or fax.
- **Check** the metadata sheet to make sure that the header information, especially author names and the corresponding affiliations are correctly shown.
- **Check** the questions that may have arisen during copy editing and insert your answers/ corrections.
- **Check** that the text is complete and that all figures, tables and their legends are included. Also check the accuracy of special characters, equations, and electronic supplementary material if applicable. If necessary refer to the *Edited manuscript*.
- The publication of inaccurate data such as dosages and units can have serious consequences. Please take particular care that all such details are correct.
- Please **do not** make changes that involve only matters of style. We have generally introduced forms that follow the journal's style. Substantial changes in content, e.g., new results, corrected values, title and authorship are not allowed without the approval of the responsible editor. In such a case, please contact the Editorial Office and return his/her consent together with the proof.
- If we do not receive your corrections **within 48 hours**, we will send you a reminder.
- Your article will be published **Online First** approximately one week after receipt of your corrected proofs. This is the **official first publication** citable with the DOI. **Further changes are, therefore, not possible.**
- The **printed version** will follow in a forthcoming issue.

Please note

After online publication, subscribers (personal/institutional) to this journal will have access to the complete article via the DOI using the URL: [http://dx.doi.org/\[DOI\]](http://dx.doi.org/[DOI]).

If you would like to know when your article has been published online, take advantage of our free alert service. For registration and further information go to: <http://www.link.springer.com>.

Due to the electronic nature of the procedure, the manuscript and the original figures will only be returned to you on special request. When you return your corrections, please inform us if you would like to have these documents returned.

Metadata of the article that will be visualized in OnlineFirst

ArticleTitle	Up-regulation of pro-angiogenic molecules and events does not relate with an angiogenic switch in metastatic osteosarcoma cells but to cell survival features	
Article Sub-Title		
Article CopyRight	The Author(s), under exclusive licence to Springer Science+Business Media, LLC, part of Springer Nature (This will be the copyright line in the final PDF)	
Journal Name		
Corresponding Author	Family Name	Bolontrade
	Particle	
	Given Name	Marcela F.
	Suffix	
	Division	Remodeling Processes and Cellular Niches Laboratory, Instituto de Medicina Traslacional E Ingeniería Biomédica (IMTIB)—CONICET—Hospital Italiano Buenos Aires (HIBA)
	Organization	Instituto Universitario del Hospital Italiano (IUHI)
	Address	Potosí 4240, C1199ACL, CABA, Argentina
	Phone	
	Fax	
	Email	marcela.bolontrade@hospitalitaliano.org.ar
	URL	
	ORCID	http://orcid.org/0000-0002-8664-5541
Author	Family Name	Gutiérrez
	Particle	
	Given Name	Luciana M.
	Suffix	
	Division	Remodeling Processes and Cellular Niches Laboratory, Instituto de Medicina Traslacional E Ingeniería Biomédica (IMTIB)—CONICET—Hospital Italiano Buenos Aires (HIBA)
	Organization	Instituto Universitario del Hospital Italiano (IUHI)
	Address	Potosí 4240, C1199ACL, CABA, Argentina
	Phone	
	Fax	
	Email	
	URL	
	ORCID	
Author	Family Name	Alvarez
	Particle	
	Given Name	Matías Valenzuela
	Suffix	
	Division	Remodeling Processes and Cellular Niches Laboratory, Instituto de Medicina Traslacional E Ingeniería Biomédica (IMTIB)—CONICET—Hospital Italiano Buenos Aires (HIBA)
	Organization	Instituto Universitario del Hospital Italiano (IUHI)

Address Potosí 4240, C1199ACL, CABA, Argentina
Phone
Fax
Email
URL
ORCID

Author Family Name **Yang**
Particle
Given Name **Yuanzheng**
Suffix
Division Division of Pediatrics and Department of Cancer Biology
Organization University of Texas M. D. Anderson Cancer Center
Address 1515 Holcombe Boulevard, Unit #853, Houston, TX, 77030, USA
Phone
Fax
Email
URL
ORCID

Author Family Name **Spinelli**
Particle
Given Name **Fiorella**
Suffix
Division
Organization CITNOBA UNNOBA
Address Jorge Newbery 261, B6000, Junín, Argentina
Phone
Fax
Email
URL
ORCID

Author Family Name **Cantero**
Particle
Given Name **María Jose**
Suffix
Division Facultad de Ciencias Biomédicas, Instituto de Investigaciones en Medicina Traslacional (IIMT), CONICET
Organization Universidad Austral
Address Pilar, Buenos Aires, Argentina
Phone
Fax
Email
URL
ORCID

Author Family Name **Alaniz**
Particle

Given Name **Laura A.**
Suffix
Division
Organization CITNOBA UNNOBA
Address Jorge Newbery 261, B6000, Junín, Argentina
Phone
Fax
Email
URL
ORCID

Author Family Name **Garcia**
Particle
Given Name **Mariana G.**
Suffix
Division Facultad de Ciencias Biomédicas, Instituto de Investigaciones en Medicina Traslacional (IIMT), CONICET
Organization Universidad Austral
Address Pilar, Buenos Aires, Argentina
Phone
Fax
Email
URL
ORCID

Author Family Name **Kleinerman**
Particle
Given Name **Eugenie S.**
Suffix
Division Division of Pediatrics and Department of Cancer Biology
Organization University of Texas M. D. Anderson Cancer Center
Address 1515 Holcombe Boulevard, Unit #853, Houston, TX, 77030, USA
Phone
Fax
Email
URL
ORCID

Author Family Name **Correa**
Particle
Given Name **Alejandro**
Suffix
Division
Organization Instituto Carlos Chagas Fiocruz/PR
Address Curitiba, 81350-010, Brazil
Phone
Fax
Email

URL
ORCID

Schedule	Received Revised Accepted 30 April 2021
Abstract	<p>Osteosarcoma (OS) is the most frequent malignant bone tumor, affecting predominantly children. Metastases represent a major clinical challenge and an estimated 80% would present undetectable micrometastases at diagnosis. The identification of metastatic traits and molecules would impact in micrometastasis management. Microvascular endothelium tube formation and in vivo angiogenesis assays, adhesion assays, apoptosis assays, proteomic analysis, RT-qPCR. We demonstrated that OS LM7 metastatic cells secretome was able to induce microvascular endothelium cell rearrangements, an angiogenic-related trait. A proteomic analysis indicated a gain in angiogenic-related pathways in these cells, as compared to their parental-non-metastatic OS SAOS2 cells counterpart. Further, factors with proangiogenic functions like VEGF and PDGF were upregulated in LM7 cells. However, no differential angiogenic response was induced by LM7 cells in vivo. Regulation of the Fas–FasL axis is key for OS cells to colonize the lungs in this model. Analysis of the proteomic data with emphasis in apoptosis pathways and related processes revealed that the percentage of genes associated with those, presented similar levels in SAOS2 and LM7 cells. Further, the balance of expression levels of proteins with pro- and antiapoptotic functions in both cell types was subtle. Interestingly and of relevance to the model, Fas associated Factor 1 (FAF1), which participates in Fas signaling, was present in LM7 cells and was not detected in SAOS2 cells. The subtle differences in apoptosis-related events and molecules, together with the reported cell-survival functions of the identified angiogenic factors and the increased survival features that we observed in LM7 cells, suggest that the gain in angiogenesis-related pathways in metastatic OS cells would relate to a prosurvival switch rather than an angiogenic switch as an advantage feature to colonize the lungs. OS metastatic cells also displayed higher adhesion towards microvascular endothelium cells suggesting an advantage for tissue colonization. A gain in angiogenesis pathways and molecules does not result in major angiogenic potential. Together, our results suggest that metastatic OS cells would elicit signaling associated to a prosurvival phenotype, allowing homing into the hostile site for metastasis. During the gain of metastatic traits process, cell populations displaying higher adhesive ability to microvascular endothelium, negative regulation of the Fas–FasL axis in the FasL (–) lung parenchyma and a prosurvival switch, would be selected. This opens a new scenario where antiangiogenic treatments would affect cell survival rather than angiogenesis, and provides a molecular panel of expression that may help in distinguishing OS cells with different metastatic potential.</p>
Keywords (separated by '-')	Osteosarcoma - Prosurvival phenotype - Apoptosis - Metastasis - Angiogenesis
Footnote Information	Supplementary Information The online version contains supplementary material available at https://doi.org/10.1007/s10495-021-01677-x .



Up-regulation of pro-angiogenic molecules and events does not relate with an angiogenic switch in metastatic osteosarcoma cells but to cell survival features

Luciana M. Gutiérrez¹ · Matías Valenzuela Alvarez¹ · Yuanzheng Yang² · Fiorella Spinelli³ · María Jose Cantero⁴ · Laura A. Alaniz³ · Mariana G. Garcia⁴ · Eugenie S. Kleinerman² · Alejandro Correa⁵ · Marcela F. Bolontrade¹

Accepted: 30 April 2021
© The Author(s), under exclusive licence to Springer Science+Business Media, LLC, part of Springer Nature 2021

Abstract

Osteosarcoma (OS) is the most frequent malignant bone tumor, affecting predominantly children. Metastases represent a major clinical challenge and an estimated 80% would present undetectable micrometastases at diagnosis. The identification of metastatic traits and molecules would impact in micrometastasis management. Microvascular endothelium tube formation and in vivo angiogenesis assays, adhesion assays, apoptosis assays, proteomic analysis, RT-qPCR. We demonstrated that OS LM7 metastatic cells secretome was able to induce microvascular endothelium cell rearrangements, an angiogenic-related trait. A proteomic analysis indicated a gain in angiogenic-related pathways in these cells, as compared to their parental-non-metastatic OS SAOS2 cells counterpart. Further, factors with proangiogenic functions like VEGF and PDGF were upregulated in LM7 cells. However, no differential angiogenic response was induced by LM7 cells in vivo. Regulation of the Fas–FasL axis is key for OS cells to colonize the lungs in this model. Analysis of the proteomic data with emphasis in apoptosis pathways and related processes revealed that the percentage of genes associated with those, presented similar levels in SAOS2 and LM7 cells. Further, the balance of expression levels of proteins with pro- and antiapoptotic functions in both cell types was subtle. Interestingly and of relevance to the model, Fas associated Factor 1 (FAF1), which participates in Fas signaling, was present in LM7 cells and was not detected in SAOS2 cells. The subtle differences in apoptosis-related events and molecules, together with the reported cell-survival functions of the identified angiogenic factors and the increased survival features that we observed in LM7 cells, suggest that the gain in angiogenesis-related pathways in metastatic OS cells would relate to a prosurvival switch rather to an angiogenic switch as an advantage feature to colonize the lungs. OS metastatic cells also displayed higher adhesion towards microvascular endothelium cells suggesting an advantage for tissue colonization. A gain in angiogenesis pathways and molecules does not result in major angiogenic potential. Together, our results suggest that metastatic OS cells would elicit signaling associated to a prosurvival phenotype, allowing homing into the hostile site for metastasis. During the gain of metastatic traits process, cell populations displaying higher adhesive ability to microvascular endothelium, negative regulation of the Fas–FasL axis in the FasL (–) lung parenchyma and a prosurvival switch, would be selected. This opens a new scenario where antiangiogenic treatments would affect cell survival rather than angiogenesis, and provides a molecular panel of expression that may help in distinguishing OS cells with different metastatic potential.

Keywords Osteosarcoma · Prosurvival phenotype · Apoptosis · Metastasis · Angiogenesis

✉ Marcela F. Bolontrade
marcela.bolontrade@hospitalitaliano.org.ar

¹ Remodeling Processes and Cellular Niches Laboratory, Instituto de Medicina Traslacional E Ingeniería Biomédica (IMTIB)—CONICET—Hospital Italiano Buenos Aires (HIBA), Instituto Universitario del Hospital Italiano (IUI), Potosí 4240, C1199ACL CABA, Argentina

² Division of Pediatrics and Department of Cancer Biology, University of Texas M. D. Anderson Cancer Center, 1515 Holcombe Boulevard, Unit #853, Houston, TX 77030, USA

³ CITNOBA UNNOBA, Jorge Newbery 261, B6000 Junín, Argentina

⁴ Facultad de Ciencias Biomédicas, Instituto de Investigaciones en Medicina Traslacional (IIMT), CONICET, Universidad Austral, Pilar, Buenos Aires, Argentina

⁵ Instituto Carlos Chagas Fiocruz/PR, Curitiba 81350-010, Brazil

A11
A12

A13
A14
A15

A16
A17

33 Introduction

34 Osteosarcoma (OS) is the most common malignant bone
 35 tumor, arising during metaphyseal rapid growth in adoles-
 36 cents and children [1]. Pulmonary metastases exist in early
 37 stages during OS progression. While lung metastases are
 38 detected in 20% of patients at diagnosis, an 80% is esti-
 39 mated to carry undetectable micrometastasis at that time
 40 [2, 3]. Patients with pulmonary metastases at diagnosis
 41 have a 25–30% five-year survival rate with no substan-
 42 tial changes in the last three decades [2, 3]. OS etiology
 43 is unclear, with osteogenic precursors accumulating not
 44 well-defined oncogenic events which hinders the use of
 45 potential markers associated to progression and metastasis
 46 [4]. Complex signaling occurs during OS onset involving
 47 a bidirectional communication between tumor cells and
 48 the bone niche. Thus, OS arises because of imbalanced
 49 bone homeostasis in the bone marrow environment. OS
 50 progression involves profound bone homeostasis deregulation,
 51 extracellular matrix remodeling and biochemical
 52 signaling that affect the stromal compartment [4]. Lungs
 53 represent the most frequent target organ for metastatic OS.
 54 Fas ligand (FasL) is constitutively expressed by alveolar
 55 and bronchial epithelial cells [5]. Our model comprises
 56 the parental, human OS Fas⁺ (CD95, APO1) SAOS2
 57 cells that are cells unable to colonize the lungs when
 58 intravenously injected into immunodeficient mice, and
 59 the SAOS2-derived LM7 cells, which are able to estab-
 60 lish secondary tumor growth into the lungs and express
 61 significantly lower Fas levels [6]. LaFleur et al. [7] have
 62 previously demonstrated that Fas⁺ OS cells are eliminated
 63 by the FasL⁺ lung epithelium while Fas⁻ OS cells escape
 64 this surveillance establishing pulmonary metastases.
 65 Thus, the gain in metastatic traits involves the absence of
 66 Fas or molecular changes necessary to downregulate its
 67 expression as a critical step in this disease. The lack of
 68 this feature turns OS cells unable to survive in the lung
 69 environment [8]. Clinical specimens corresponding from
 70 OS lung metastases express inappreciable Fas levels, while
 71 the primary bone tumor counterpart was demonstrated to
 72 express high Fas levels, making this model clinically rel-
 73 evant to understand underlying mechanisms that favor OS
 74 cells colonization into the lungs and allowing the search
 75 for novel therapeutic approaches [6]. Further, the complex
 76 modifications in the stromal primary tumor compartment
 77 could consequently exert a selection pressure over previ-
 78 ously residing OS subpopulations with differential abili-
 79 ties, thus favoring cells with metastatic traits to *leave the*
 80 *nest* towards future pulmonary metastatic sites [9]. Metas-
 81 tasis results in a complex process, with variable routes
 82 and interlinked steps [10, 11]. For metastasis to occur, the
 83 tumor cell must leave the primary site, intravasate, adhere

at the metastatic site and left the circulatory system by
 extravasation [12]. Requirements for this are a microvessel
 network, and the ability of the tumor cell to survive both
 in the circulation and at the target site [13].

Angiogenesis is a multistep process constituting the angi-
 ogenic cascade, involving complex signaling among several
 participating actors, inducing the formation of new vessels
 from preexisting ones. This process includes the degrada-
 tion of the basal membrane mediated by proteolytic enzymes
 like metalloproteinases and cathepsins, and the proliferation
 and migration of endothelial cells (ECs), followed by the
 proliferation and differentiation/maturation of ECs [14]. The
 last step involves other cellular populations, pericytes and
 smooth-muscle cells, which are recruited by the new vessel
 stabilizing it. Angiogenesis is mediated by the coordinated
 action of various cytokines and growth factors. Angiogenic
 factors such as platelet-derived growth factors (PDGFs) and
 vascular endothelial growth factor (VEGF) are necessary for
 the establishment of new vessels in physiological conditions
 and in tumors [15, 16].

We demonstrated that critical steps and events related to
 the angiogenic cascade like EC re-organization, and biolog-
 ical pathways and processes like VEGF and PDGF signaling
 were upregulated in metastatic OS cells secretome. How-
 ever, this did not result in a net differential vascular bed
 formation distinguishing metastatic from non-metastatic
 cells. Given that molecules associated with the identified
 gene ontology (GO) terms through a proteomic approach
 such as VEGF, PDGF, endothelins, are also related to sur-
 vival features, we further analyzed the proteomic data with
 emphasis in prosurvival related proteins and other molecules
 arose as relevant. Given our results, we conclude that even
 when angiogenesis is a tumor-progression associated feature
 and a tumor cannot develop without this, the process itself
 and the molecular functions associated with it, would not
 be determinant in the lung metastatic features in OS, but
 instead, a prosurvival function of these molecules would
 allow OS cells to colonize a hostile environment surviving
 the adverse circulation. This finding shed light into multiple
 functions for a given molecule/les, a feature that adds com-
 plexity and multiple advantages to a given tumor to progress.

Cancer progression involves multistep functional events,
 which may ultimately lead to the acquisition of a metastatic
 phenotype [17]. We describe for the first time a functional
 and molecular comparison between a parental non-metas-
 tatic OS cell line and its derived cell line selected by its
 metastatic behaviour, highlighting a differential molecular
 pattern that may relate to angiogenic induction potential but
 also to favour survival in a hostile environment, such as the
 pulmonary metastatic niche. Pulmonary metastases remain
 as a major OS mortality determinant, and identification of
 mechanisms and differentially expressed genes associated

136 with metastasis would help in discovering promising mark-
 137 ers and targets for therapeutic approaches for OS metastatic
 138 spread.

139 Materials and methods

140 Cell lines

141 SAOS2 and LM7 cells human OS cell lines were supplied by
 142 Dr. Kleinerman, MD Anderson Cancer Center (MDACC).
 143 Cells were grown in Dulbecco's Modified Eagle Medium:
 144 Nutrient Mixture F12 (DMEM:F12) supplemented with
 145 non-essential amino acids (NEAA), 2 mM L-glutamine,
 146 100U/mL penicillin, 100 mg/mL streptomycin (Invitrogen),
 147 10% fetal bovine serum (FBS; Natocor), at 37 °C, 5%CO₂.
 148 SAOS2 are OS cells that do not possess the capacity to form
 149 secondary tumor growth sites in the lungs, while LM7 cells
 150 have been selected from parental SAOS2 cells by their meta-
 151 static ability through lung cyclic circulation, ability asso-
 152 ciated to avoidance of apoptosis and apoptosis-resistance
 153 mechanisms [6, 18]. Human Microvascular Endothelial cells
 154 HMEC-1 (Dr. Candal, Centers for Disease Control, Atlanta,
 155 GA, USA) were grown in high-glucose DMEM (DMEM
 156 high, Invitrogen), 10% FBS (Natocor), 2 mM L-glutamine,
 157 100U/mL penicillin, and 100 mg/mL streptomycin [19]. Ver-
 158 ification of mycoplasma species was carried out (MycAlert
 159 Mycoplasma Detection Kit, Lonza Inc.).

160 Cell conditioned medium

161 The cells' secretome compartment is represented by their
 162 conditioned medium (CM). Cells were seeded on 100 mm
 163 culture dishes until 80% confluence, washed with phosphate
 164 basic solution (PBS) and cultured during twenty-four hours
 165 with basal medium (DMEM:F12). After this, the CM was
 166 collected, centrifuged for 5 min (1100 rpm), aliquoted and
 167 stored at -80 °C until use.

168 Tube formation assay

169 Tube formation was assayed using Geltrex® LDEV-Free
 170 reduced growth factor (GF) basement membrane matrix
 171 (ThermoFisher). Forty µL Geltrex/well were seeded in
 172 96-well plates (JET Bio-Filtration) allowing polymerization
 173 (37 °C, 30 min). HMEC-1 cells (2×10^4 , FBS-starved during
 174 24 h) were seeded on 50 µL of FBS free DMEM high and
 175 stimulated with CM (50 µL) from SAOS2 and LM7 cells
 176 (6 h, 37 °C). After this, cells were fixed (2% PFA) three pic-
 177 tures were taken from every well to allow for quantification
 178 (100× magnification (10× objective/10× eyepiece), Nikon).

The number of loops/well was quantified using Image J soft-
 ware, NIH, MD).

In vivo angiogenic assay

182 Animal experiments were approved by the Institutional Ani-
 183 mal Care and Use Committee (MDACC IACUC #00001633-
 184 RN00). For in vivo angiogenesis assay, athymic male nude
 185 mice were subcutaneously (s.c., right flank, midline sec-
 186 tion) injected with a pre-mixed solution of SAOS2 or LM7
 187 cells in Geltrex® LDEV-Free reduced GF basement mem-
 188 brane matrix (5×10^5 cells/40 µL PBS/500 µL Geltrex).
 189 One week after inoculation, plugs were excised, fixed (PFA
 190 4%), embedded in Optimal cutting temperature compound
 191 (OCT), frozen (liquid nitrogen) and processed for cryostat
 192 sectioning. CD31 was detected using rat anti-mouse CD31
 193 (BD Biosciences PharMingen, San Diego, CA, USA) as pri-
 194 mary antibody and goat anti-rat Texas Red (Jackson Immuno-
 195 Research, PA, USA) as secondary antibody. Nuclei were
 196 stained using Hoechst 33342 solution (1 µg/mL in PBS,
 197 Sigma) [20, 21]. Microvessel density was assessed as previ-
 198 ously described by Weidner et al. [22], briefly microvessel
 199 density was analyzed in areas with high density of capillaries
 200 and small venules (vascular "hotspots") and microvessels
 201 were counted at 200× magnification fields. Any endothelial
 202 cell cluster or vessel positive for CD31 and clearly sepa-
 203 rated from an adjacent capillar was considered to be a single
 204 microvessel [23, 24].

Cell adhesion assay

205 HMEC-1 cells were seeded at 2×10^5 cells/96-well, allow-
 206 ing the establishment of a monolayer. OS cells were stained
 207 with DiO (fluorescent cell tracker, Molecular Probes) to
 208 allow visualization; 5.0×10^3 DiO⁺ cells were seeded over
 209 the microvascular endothelium monolayer. Cell adhesion
 210 was allowed (30 min, 37 °C). Attached cells were fixed (4%
 211 PFA), visualized (fluorescence microscope, Nikon) and five
 212 representative visual fields were counted at 100× (DiO⁺
 213 cells, ImageJ software, NIH, MD, USA) [25]. The micro-
 214 vascular endothelium cell line was used as it was shown
 215 to be of clinical relevance in experimental approaches [26,
 216 27]. Disrupted microvascular endothelium areas were not
 217 included.
 218

Acridine orange/ethidium bromide (AO/EB) fluorescence staining

221 OS cell lines were cultured in culture medium with 2,5% or
 222 without FBS at 37 °C in a 4% CO₂ atmosphere and apopto-
 223 sis was evaluated at 6 h. Morphological changes associated
 224 with apoptosis were assessed by acridine orange-ethidium

225 bromide mixture staining (Sigma). Briefly, cell pellets were
 226 resuspended in dye mix (100 µg/mL acridine orange plus
 227 100 µg/mL ethidium bromide in PBS) and visualized by
 228 fluorescence microscopy (Nikon Eclipse E800). A mini-
 229 mum number of 200 cells were counted and the number of
 230 cells presenting fragmented nuclei, enlarged cytoplasm and
 231 condensed chromatin were determined. The percentage of
 232 apoptotic cells was calculated as total number of cells with
 233 apoptotic nuclei/total number of cells counted × 100 as pre-
 234 viously described [28].

235 Chromatin condensation assay

236 OS cell lines were grown on gelatin-coated glass cover-
 237 slips, with basal medium in the presence or absence of dox-
 238 orubicin (0,1 and 1 µM) and chromatin condensation and
 239 nuclear fragmentation was evaluated at 24 h after treatment.
 240 Cells were washed with PBS and fixed with 4% PFA. As
 241 previously described, nuclei were stained with 0.01 mg/mL
 242 Hoechst 33342 (15 min) to allow for nuclear morphology
 243 visualization at 100× and 400× magnification (10× and 40×
 244 objective/10× eyepiece, Nikon Eclipse E400 fluorescence
 245 microscope) [29].

246 Reverse transcription-polymerase chain reaction 247 (RT-qPCR) and real Time polymerase chain reaction 248 (qPCR)

249 Total RNA from OS cells (Trizol Reagent, Molecular
 250 Research Center, USA) was reverse transcribed (2 µg) with
 251 200 U of *EasyScript* Reverse Transcriptase (Transgenbio-
 252 tech) using Oligo (dT) primers (500 ng). cDNAs were sub-
 253 jected to qPCR (CFX96 Touch TM Real-Time PCR Detec-
 254 tion System, Bio-Rad). Fas-associated factor 1 (FAF1),
 255 VEGF, PDGFA, PDGFB, PDGFC, PDGFD, mRNA levels
 256 were quantified (SYBR Green, Roche) using the primers:
 257 FAF1 forward 5' GACCAGCTTTGGAGCTCTTG3',
 258 reverse 5' TGCGGGAAATAAAGATCTGG3'; VEGF
 259 forward 5'ATCTTCAAGCCATCCTGTGTGC 3', reverse
 260 5'GCTCACCGCCTCGGCTTGT 3'; PDGFA forward 5'
 261 CCTGCCCATTCGGAGGAAGAG 3', reverse 5' TTG
 262 GCCACCTTGACGCTGCG 3'; PDGFB forward 5' TCC
 263 CGAGGAGCTTTATGAGA 3', reverse 5' ACTGCACGT
 264 TGCGGTTGT 3'; PDGFC forward 5' GGAGCACCATGA
 265 GGAGTGTGA 3', reverse 5'GAGCTGCTGGTGGTGTATG
 266 C 3'; PDGFD forward 5' CCCAGGAATTACTIONCGGTCAA
 267 3', reverse 5' ACAGCCACAATTTCTCCAC 3'. PCR
 268 amplification was carried out using a 95 °C for 10 min
 269 cycle and 40 cycles under the parameters: 95 °C for 20 s,
 270 60 °C for 1 min, 72 °C for 40 s and a 95 °C for 20 s cycle.
 271 At the end the temperature was increased from 60to 95 °C
 272 (2 °C/min rate), and fluorescence was measured every 15 s

to construct the melting curve. Values were normalized
 to levels of glyceraldehyde-3-phosphate dehydrogenase
 (GAPDH) mRNA levels, forward 5' GGGGCTGCCAG
 AACATCAT 3', reverse 5' GCCTGCTTACCACCTTC
 TTG 3'. Data were processed by the DDCT method. A non-
 template control (NTC) was run in every assay; all deter-
 minations were performed as triplicates in three separated
 experiments.

281 Proteomics and proteomic data analysis

282 To analyzed the proteomic profile of the cellular and
 283 secretome components of OS tumor cells, cell pellets
 284 (4 × 10⁷ cells) and CM (12 mL) were lyophilized for stor-
 285 age and transport. Later, samples were resuspended in lysis
 286 buffer (100 mM Tris-HCl, pH 7.5, 4% SDS, 100 mM DTT
 287 and H₂O 18.2 MΩ cm at a ratio of 1:1 (v/v) for 15 min at
 288 94 °C. The samples were subjected to sonication (30 min),
 289 centrifuged at 16,000×g for 5 min and separated by 10%
 290 SDS-PAGE. Once the electrophoretic run was finished, the
 291 gel was stained with Coomassie blue and the lanes were
 292 excised and cut into small pieces of equal size and treated
 293 with trypsin. The resulting peptides were processed, and
 294 analyzed with a tandem system of nanocapillary liquid
 295 chromatography-mass spectrometry (Thermo Scientific
 296 Easy-nLC 1000 system connected to an LTQ Orbitrap XL
 297 ETD) as previously described [30].

298 For the identification, quantification (label free) and
 299 validation of the proteins, the MaxQuant platform (ver-
 300 sion 1.5.2.8) was used, which includes the Andromeda
 301 algorithm for database search. Uniprot was the database
 302 used for protein search and complemented with the elimi-
 303 nation of frequent contaminants (porcine trypsin) and
 304 also reverse sequences. To validate the assigned protein
 305 identity, a minimum of seven amino acids was established
 306 for each peptide and a Q value cut-off of 0.01 was also
 307 established at the level of peptides and proteins [30, 31].
 308 To obtain the gene ontology terms (GO) of the identified
 309 proteins, an enrichment analysis was carried out with the
 310 software Funrich, of the gene groups corresponding to the
 311 secretome and the intracellular compartment. To select the
 312 categories with statistical significance, p values were taken
 313 at 0.05. The focus was on the analysis of GO terms related
 314 to angiogenesis, survival and processes related to angio-
 315 genic potential. To assess relative expression of individual
 316 proteins in each compartment, a label free approach was
 317 performed as previously described. The normalized label
 318 free quantification (LFQ) protein values were expressed
 319 as relative intensity values and for normalization the LFQ
 320 media intensity of all proteins were used. LFQ (Label-free
 321 quantification) intensities are based on the (raw) intensities
 322 (sums of all individual peptide intensities, peaks in a MS

323 spectra, belonging to a particular protein) and normalized
324 on multiple levels to ensure that profiles of LFQ intensities
325 across samples reflect the relative amounts of the proteins.
326 [30].

327 Database search

328 Data about the expression of PDGFA, PDGFB, PDGFC,
329 PDGFD, VEGF and FAF1 in OS samples were obtain from
330 the Gene Expression Omnibus (GEO) database number
331 GSE42352. The data set called mixed Osteosarcoma-Kuiper-
332 127-vst-ilmnhwg6v2 data set, has 127 samples originally.
333 Genome-wide gene expression analysis was performed using
334 pretreatment high-grade diagnostic OS biopsy samples. The
335 R2: Genomics analysis and visualization platform ([http://r2.
336 amc.nl](http://r2.amc.nl)) was used to generate Kaplan–Meier metastasis-free
337 survival curves, omitting from the analysis 39 samples that
338 lacked survival data.

339 Statistical analysis

340 Ninety-five percent (95%) of confidence intervals (CI)
341 were determined by calculating arithmetic mean values
342 and variance (standard deviation, SD) of three independent
343 experiments. Unpaired 2-sided Student's t test (two groups
344 comparisons) and analysis of variance (ANOVA) followed
345 by post-tests Kruskal–Wallis and Dunn's post-tests (more
346 than two experimental groups comparisons) (GraphPad
347 Prism Software, San Diego, CA, USA) were used for sta-
348 tistical analyses, considering p value < 0.05 as statistically
349 significant.

350 Results

351 Microvascular endothelium cells rearrangements 352 and in vivo angiogenic response induced by OS cells

353 Neovessel formation, which is associated with cancer pro-
354 gression in a variety of tumor models, involves the coordi-
355 nated occurrence of several steps leading to new functional
356 vessels. We evaluated the capacity of SAOS2 and LM7 OS
357 cells secretome to exert morphogenic rearrangements in
358 microvascular endothelium cell monolayers, a step associ-
359 ated to the angiogenic cascade. To this end we performed
360 in vitro tube formation assays on HMEC-1 cells. LM7 cells
361 secretome resulted as the major tube inducer as compared to
362 the tube-inducing capacity of parental cells secretome, basal
363 medium and serum-supplemented basal medium, producing
364 a 1.3-fold increase in microvascular endothelium cell rear-
365 rangement as compared to the response exerted by SAOS2

366 cells (Fig. 1a, b). When in vivo angiogenesis assays were
367 performed with OS cells, the density of CD31⁺ microves-
368 sels induced by SAOS2 and LM7 cells were similar. Further,
369 no qualitative differences were observed in the vasculature
370 induced by OS cells (Fig. 1c, d).

371 Osteosarcoma cells adhesive behavior 372 towards microendothelium

373 Cell adhesion to endothelium is critical for intravasation
374 and extravasation during the metastatic cascade. We ana-
375 lyzed the adhesive behavior of OS cells to microvascular
376 endothelium cells (HMEC-1) and also analyzed proteomic
377 data with emphasis on proteins related to adhesion. To this
378 end, SAOS2 and LM7 cells were subjected to an adhesion
379 assay on HMEC-1 cells. We observed that LM7 cells dis-
380 played significantly higher adhesiveness to HMEC-1 cells
381 (30 min, 1.6-fold increase, Fig. 2a, b). Proteomic analysis
382 with emphasis in adhesion-related molecules, revealed that
383 both cell lines expressed proteins implicated in this biologi-
384 cal process like integrins, catenins and cell adhesion mol-
385 ecules (CAM). Analysis of protein relative levels revealed
386 an overall higher expression of adhesion related proteins in
387 SAOS2, with LM7 cells expressing high levels for ALCAM
388 (activated leukocyte cell adhesion molecule, Fig. 2c).

389 Expression of molecules related to angiogenesis 390 and pro-survival signaling pathways

391 Analysis of biological pathways indicated that PDGF signal-
392 ing was increased in LM7 cells. PDGF was demonstrated to
393 have angiogenic and cell-survival properties [32]. Validation
394 through qPCR indicated an eightfold and threefold increase
395 for PDGFB and D respectively in LM7, with no appreci-
396 able differences in PDGFA and C expression (Fig. 3a). We
397 observed a gain in biological pathways associated with
398 angiogenesis (PECAM1 interactions, VEGF and VEGF
399 receptor signaling, endothelins, integrins in angiogenesis
400 and angiopoietin receptor tie2 mediated signaling among
401 others) (Supplementary material Table 1), but a lack of a
402 net in vivo angiogenic response difference between the cell
403 types (see Fig. 1). Of interest, expression analysis of VEGF,
404 a factor with pro-angiogenic and pro-survival reported func-
405 tions [33], showed a twofold increase in expression by qPCR
406 in LM7 cells (Fig. 3b). Given that apoptosis and cell sur-
407 vival exert a role in this model, these results could point to a
408 scenario where PDGF and VEGF would be related to their
409 reported cell-survival functions rather than to a differential
410 angiogenic response. Further, of the exclusive LM7 proteins
411 identified, FAF1, a FAS interactor [34], (see in "Proteomic
412 analysis of apoptosis pathway and related processes" sec-
413 tion) demonstrated a 17-fold expression increase in LM7
414 cells as compared to their non-metastatic counterpart

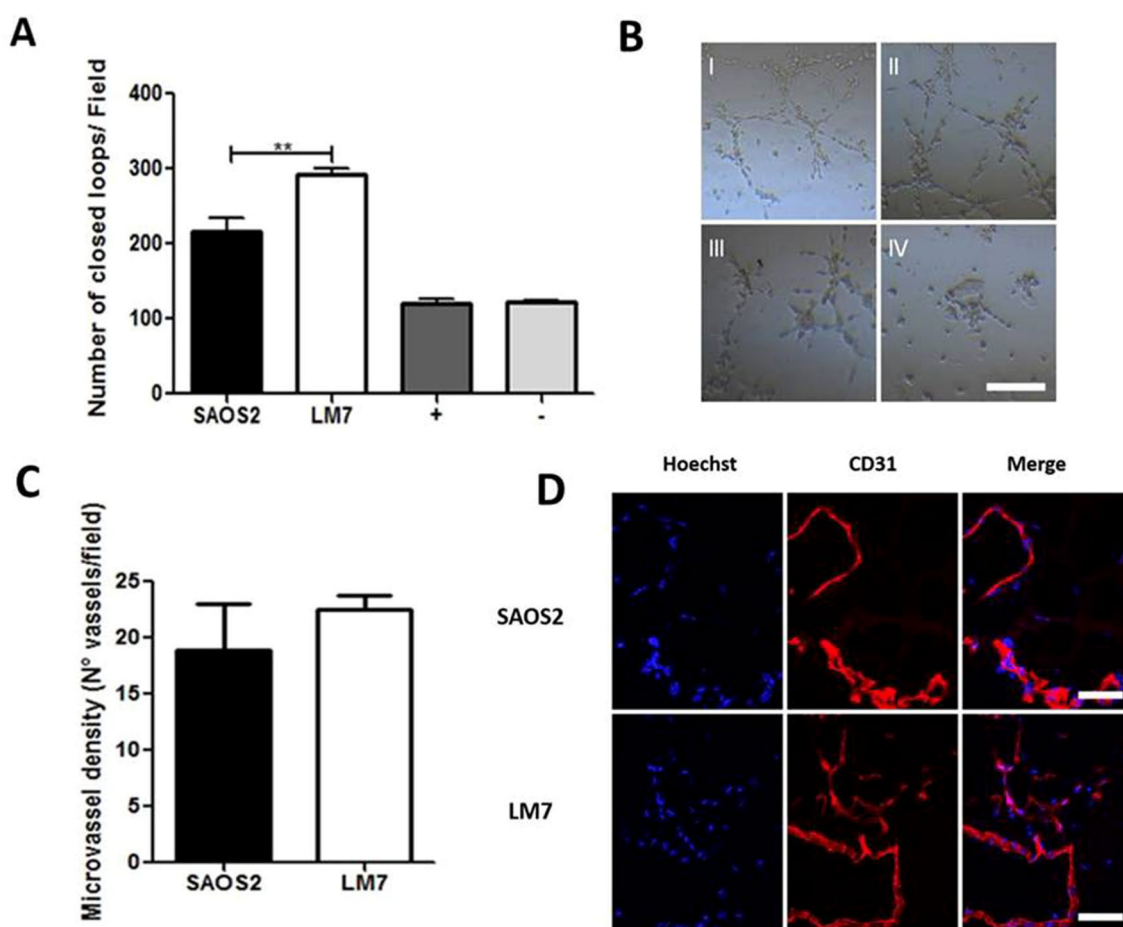


Fig. 1 Angiogenic effect exerted by OS human cells or their secretome. **a** In vitro tube formation assay to test the ability of OS cells secretome to induce morphogenic rearrangements. HMEC-1 microvascular endothelium cells were treated with SAOS2 (parental cells) or LM7 cells-derived conditioned medium (CM). DF12 supplemented with 10% FBS and DF12 basal medium were used as positive (+) and negative (-) stimuli, respectively. One-way ANOVA, ** $p < 0.01$. Data are representative of three independent experiments. **b** Representative images of in vitro tube formation assays with

SAOS2 or LM7-derived CM; (i) HMEC-1 cells treated with SAOS2 CM; (ii) HMEC-1 cells treated with LM7 CM; (iii) HMEC-1 cells treated with DF12 medium with 10% FBS; (iv) HMEC-1 cells with DF12 basal medium. Scale bar represent 0.2 mm. (C) In vivo angiogenesis assay with Geltrex plugs containing SAOS2 or LM7, showing the quantification of microvessel density by CD31⁺ microvessels detection after 7 days. (D) Representative images of the plugs of the in vivo angiogenesis assay. Nuclei were stained with Hoechst and vessels detected with CD31 antibody. Scale bar represent 50 μ m

415 (Fig. 3c). We complemented this data by analyzing a
416 genome-wide gene expression dataset (The R2: Genomics
417 Analysis and Visualization Platform) of high grade OS pre-
418 chemotherapy biopsies (88 pre-treatment high-grade osteo-
419 sarcoma diagnostic biopsies). Of relevance, we observed that
420 PDGF isoforms, FAF1 and VEGF shared a common feature
421 in patients, with higher expression of these proteins related
422 with a worst overall survival as confirmed by Kaplan–Meier
423 curves (Supp. Figure 1).

424 Proteomic analysis of apoptosis pathway 425 and related processes

426 Apoptosis is a cell death mechanism, where a cascade of
427 mediators triggered by different ligand mediated signals

like Fas/FasL, induce the release of caspases from the 428
mitochondria and conclude in cell death. Since our model 429
involves a Fas⁺ SAOS2 and Fas⁻ LM7 cell model, which 430
allows LM7 cells to survive in the FasL⁺ lung parenchyma 431
[6], we analyzed our proteomic data with emphasis in 432
apoptosis pathways and related processes. The percent- 433
age of genes associated with apoptotic signaling path- 434
ways, apoptotic processes in general and regulation of 435
apoptotic processes presented similar levels in SAOS2 and 436
LM7 cells (Table 1). Interestingly and of relevance to the 437
model, when looking into proteins associated to apoptosis, 438
Fas associated Factor 1 (FAF1), which participates as an 439
enhancer of Fas signaling [34, 35], was present in LM7 440
cells (2,876200e+007, normalized LFQ value) and was 441
not detected in SAOS2 cells, which was validated through 442

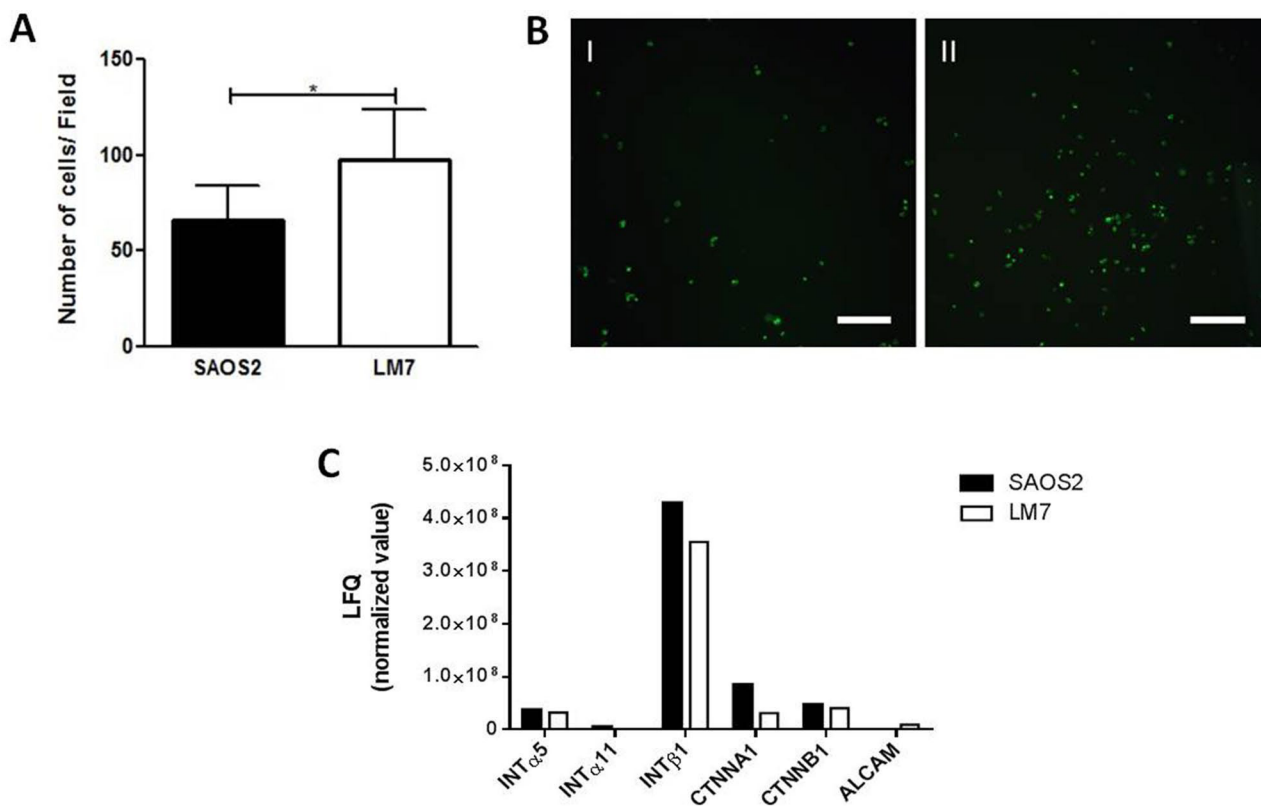


Fig. 2 Osteosarcoma cells adhesive behavior to microvascular endothelium. **a** Adhesion of SAOS2 and LM7 cells on HMEC-1 cells monolayers at 30 min, represented as number of cells per field. *t* test, **p* < 0.05. **b** Representative pictures of SAOS2 cells (panel I) and LM7 cells (panel II) stained with DiO, over the HMEC-1 monolayer. Pictures were taken at $\times 100$, with fluorescence microscope to allow visualization of pre-labelled OS cells. Scale bar represents 0.2 mm. Data

and images are representative of three independent experiments. **c** The graph bars show the LFK normalized values of adhesion-related proteins identified by analysis with Funrich program, for both OS cell lines proteomes. INT α 5: integrin alpha 5; INT α 11: integrin alpha 11; INT β 1: integrin beta 1; CTNNA1: catenin alpha 1; CTNNB1: catenin beta 1; ALCAM: activated leukocyte cell adhesion molecule. Notably, ALCAM was only present in LM7 cells

443 qPCR, with LM7 showing significantly higher levels of
 444 expression as compared to SAOS2 cells (see Fig. 3c).
 445 The balance of expression levels of other proteins with
 446 pro- and antiapoptotic functions in both cell types was
 447 subtle, with SAOS2 displaying higher expression of the
 448 proapoptotic BAG2 and BAG6 and of the antiapoptotic
 449 AATF, BCL2L13 and API5 molecules, while LM7 showed
 450 increased expression of the proapoptotic BLAF1, AIFM1
 451 and CASP3, and of the antiapoptotic BAG3 and BAG5
 452 proteins (Supplementary material table 2). The subtle
 453 differences in apoptosis-related events and molecules
 454 together with our previous results showing that LM7 are
 455 more resistant than SAOS2 cells to cytotoxic agents like
 456 doxorubicin [36], could suggest that cell survival-related
 457 mechanisms would be of relevance in this model. Inter-
 458 estingly, under starvation conditions SAOS2 cells had a
 459 6.3-fold increase in apoptosis levels (without FBS sup-
 460 plementation), and a 6.0 fold increase in apoptosis with
 461 2.5% FBS supplementation, as compared to LM7 cells
 462 (Fig. 4a). After treatment with 0.1 and 1 μ M doxorubicin

for 24 h, an increasing number of SAOS2 cells started to
 display nuclear features compatible with apoptotic cells,
 like chromatin condensation or nuclear fragmentation,
 while LM7 cells showed similar levels of apoptotic-like
 nucleus in the control and treated groups as compared to
 SAOS2 (Fig. 4b).

Discussion

Despite therapeutic combinations, the five-year survival rate
 for OS remains in 60–70%, and patients with pulmonary
 metastases at diagnosis present a 25–30% five-year survival
 rate for the last thirty years [3]. Human OS LM7 cells, which
 are able to establish secondary tumor growth into the lungs
 and express significantly lower Fas levels, are derived from
 the non-metastatic, Fas⁺ SAOS2 cells [6]. Fas⁺ OS cells
 are eliminated by the FasL⁺ lung environment and Fas⁻ OS
 cells are able to establish pulmonary metastases as previ-
 ously demonstrated in this model [7]. Of relevance, this has

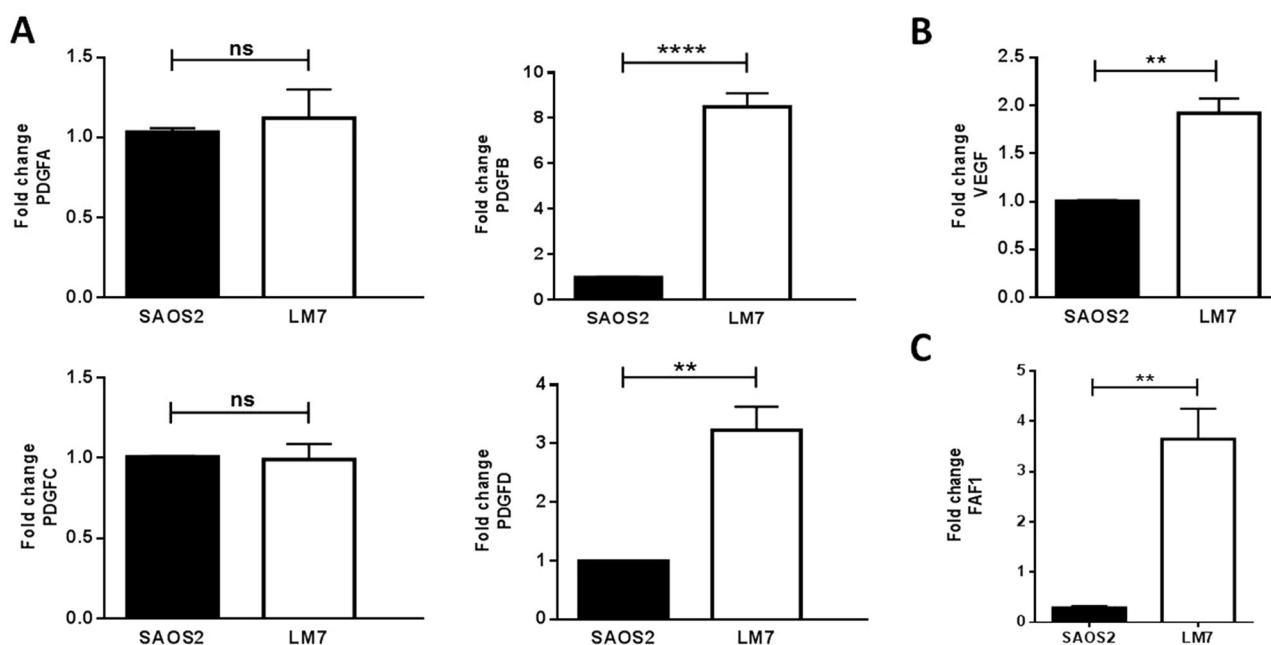


Fig. 3 RT-qPCR analysis of OS human cells. **a** PDGFA, PDGFB, PDGFC and PDGFD. **b** VEGF and **c** FAF1. The results represent the average expression + SD. PDGFA: platelet derived growth factor A; PDGFB: platelet derived growth factor B; PDGFC: platelet derived

growth factor C; PDGFD: platelet derived growth factor D; VEGF: vascular endothelial growth factor; FAF1: Fas-associated protein 1. *t test*, ns not significant; ** $P < 0.01$; **** $P < 0.0001$. Data are representative of three independent experiments

Table 1 OS cells apoptosis pathway and related processes

Biological process	SAOS2			LM7		
	Percentage of genes	Fold enrichment	P-value	Percentage of genes	Fold enrichment	P-value
Negative regulation of apoptotic process	4.78	1.76	***	4.59	1.69	***
Positive regulation of apoptotic process	2.72	1.51	**	2.77	1.53	**
Regulation of apoptotic process	1.60	1.38	ns	1.53	1.32	ns
Apoptotic signaling pathway	0.46	1.41	ns	0.51	1.54	ns
Apoptotic process	3.39	1.09	ns	3.57	1.15	ns

Percentage of genes represent the relation between the number of expressed genes related to a specific GO term and the number of genes of the GO. Fold enrichment represents the comparison between the frequency of genes annotated in a specific GO term against the frequency of genes that fall into the same GO term. Analyses considering the relative abundance of the proteins (LFQ normalized intensities) were carried out using Funrich software

LFQ label free quantification, GO gene ontology, Ns not significant

** $p < 0.01$; *** $p < 0.001$

480 a relationship with clinical observations, with the primary
481 OS tumor expressing high Fas levels and inappreciable Fas
482 levels in OS lung metastases [6]. The tumor niche is estab-
483 lished through the interplay between tumor cells, cancer
484 stem cells, stromal cells and the extracellular matrix [37,
485 38], and the use of this clinically relevant model would help
486 in addressing fundamental mechanisms that allow for OS
487 lung metastasis establishment.

488 Tumor progression is a complex biological process that
489 involves a gain in several biological mechanisms such as
490 angiogenesis, adherence, and cell survival, among others.
491 In order to elucidate if metastatic abilities acquired and/
492 or selected in LM7 cells were accompanied with other
493 hallmarks, we performed functional assays and analyzed
494 proteomic data with emphasis on biological pathways and
495 processes involved in the different functional abilities that

OS cell types evaluated, without a significant net balance in either cell type, cell protective effects exerted by PDGF and VEGF could be counteracting pro-apoptotic effects and thus promoting OS LM7 cell survival. It was demonstrated that the activation of caspase 3 was significantly reduced by PDGF-BB pretreatment in cells challenged with gp120 [55] and VEGF was shown to promote cell survival through the inhibition of caspase 3 cleavage [56]. In this regard, the significant higher expression levels of caspase 3 in LM7 cells, despite cell-death resistant features observed in these cells, could be related to signaling through PDGF and VEGF promoting a switch to cell survival despite the presence of pro-apoptotic proteins. As mentioned, OS metastasizes predominantly to the lungs emphasizing the importance of the microenvironment. Associated to its function, lungs are very well vascularized [57, 58], and although there are reports of angiogenic-independent tumor growth in this organ [59, 60], in OS the high vascularization in the lungs may provide a suitable scenario where molecules like VEGF and PDGF would switch into a pro-survival function rather to a pro-angiogenic function. Our results showed that PDGFB and PDGFD were upregulated members of the PDGF family (see Fig. 3). Of interest, analysis of metastasis-free survival data of OS patients revealed that both PDGF isoforms upregulated in our model, were of importance in a clinical scenario, with high expression associated to worst overall survival as confirmed by Kaplan–Meier curves (Supplementary material Fig. 1). Pertinent to this, there is a correlation between PDGF and VEGF networks, exemplified in the potent VEGF secretion induced by PDGF-B in an ovarian cancer model [61]. Of relevance, Langley et al. [62] have demonstrated that the PDGFBB isoform functions as a survival factor for bone-derived microvascular endothelial cells. Cell stress conditions can lead to cell survival or to cell death [63]. In this regard we showed that LM7 cells were more resistant to apoptosis under starvation conditions (see Fig. 4a), and doxorubicin treatment induced in LM7 cells diminished nuclear features compatible with apoptosis (see Fig. 4b). In this context we have recently shown that OS metastatic cells have an increased capacity to modify the intracellular localization of chemodrugs, further emphasizing the idea of a gain in pro-survival mechanisms in LM7 cells [36]. Worth mentioning in this scenario, the angiogenic-related endothelins that we identified in pathways upregulated in LM7 cells, have also been reported as multifunctional proteins with prosurvival and chemoprotective properties [64, 65]. Altogether, our results suggest that augmented PDGF and VEGF could relate, in metastatic OS cells, to signaling carrying increased surviving properties. Relevant to the model, when looking into proteins associated to apoptosis, the Fas signaling enhancer FAF1 protein was expressed in high levels in LM7 cells (see Fig. 3). Initially recognized as a member of the FAS death-inducing signaling complex,

subsequent work revealed FAF1 functions in diverse biological processes, playing an important role in development and neural survival [34], thus adding to pro-survival features. Recent evidence shows that AKT can induce FAF1 phosphorylation through the action of growth factors or oncogenic mutations, ultimately inducing pro-metastatic functions induced by TGF- β [66]. FAF1 overexpression in pre-osteoblastic cells resulted in suppression of endogenous Wnt-induced genes and decreased osteoblast differentiation, and in relation with this our group has reported that LM7 cells present lower osteoblastic differentiation potential in contrast to SAOS2 cells [36, 67]. This evidence poise a novel advantage for FAF1 expressing OS cells irrespective of its role in the FAS-mediated apoptosis response and adds to the picture as a possible regulator of tumor cells survival upon lung arrival.

We demonstrated an increase in cell adhesion towards microvascular endothelium in LM7 cells. Proteomic analysis revealed that both cell types expressed proteins associated with this biological process like integrins, catenins and cell adhesion molecules (CAM), with protein relative levels overall higher in SAOS2. This would point to a higher adhesive behavior of non-metastatic cells at a primary tumor site, but the selective advantage of metastatic cells to highly adhere to endothelium would relate to the ability of being retained in the lung' microvessels and to colonize the target site [68]. Of interest, ALCAM, a molecule involved in mechanisms associated to cell intravasation was identified as an upregulated protein in metastatic cells (see Fig. 2c), supporting this notion. Further, ALCAM was associated to metastasis to bone in a primary prostate model, associating an antiapoptotic function to this protein based on the intracellular signaling that implicates ALCAM [69]. Relevant to a role in metastases, antibody neutralization of ALCAM was demonstrated to significantly reduce tumor cells colonization into the brain using metastatic breast carcinoma models [70], and the expression of this molecule could relate to an overall function in favoring migration of mobile cells like metastasizing cells, mediating cell–cell-interactions in general [71].

From our results, a picture emerges that depicts a heterogeneous OS tumor site of pathologic bone remodeling with selection of advantageous properties in bone residing cells allowing lung colonization. An overall molecular balance may shift into one or the other side of survival or death, which may co-occur independently of the presence or absence of Fas. We identified proteins that are pro-apoptotic in a context where Fas is present like FAF1, but its participation also in prosurvival pathways could present a scenario in which not only Fas negative OS cells could colonize the lungs. To our knowledge, this notion is novel and little explored, deserving more investigation to allow for the manipulation of the permissive soil for metastasis to occur.

660 Interestingly, Kaplan–Meier curves for FAF1 predict that
 661 a higher expression is associated to lower metastasis-free
 662 survival (Supplementary material Fig. 1). A pathological
 663 analysis involving new vessel formation would not be clinically
 664 useful as indication of metastatic potential. Further,
 665 a molecular pattern associated to apoptosis and survival
 666 was presented in cells with divergent metastatic potential.
 667 Identification of novel molecules in OS cells with metastatic
 668 features would allow for a prompt validation of molecules
 669 with biomarker usefulness in a disease where the existence
 670 of non-detectable lung micrometastases remains as a critical
 671 clinical challenge.

672 Availability of data

673 The authors confirm that the data supporting the findings of
 674 this study are available within the article or its supplementary
 675 information.

676 **Supplementary Information** The online version contains supplementary
 677 material available at <https://doi.org/10.1007/s10495-021-01677-x>.

678 **Acknowledgements** We thank the Program for Technological Development
 679 in Tools for Health-PDTIS-FIOCRUZ for the use of the mass
 680 spectrometry facility.

681 **Author contributions** LMG and MVA performed experiments, analyzed
 682 data and designed figures; FS, MJ., MGG and YY performed
 683 experiments; AC conducted proteomic analysis and analyzed data;
 684 ESK, MGG and LA contributed with essential reagents and analyzed
 685 data; ESK provided OS cells. ESK and AC contributed with paper
 686 revision; MB conceived research and experiments and analyzed data.
 687 Authors discussed and commented the results on the manuscript.

688 **Funding** This work was supported by grants from the Agencia
 689 Nacional de Promoción Científica y tecnológica (ANPCyT) PICT
 690 N°1974.

691 Declarations

692 **Conflicts of interest** Authors declare that no competing financial interests
 693 or conflicts of interest exist.

694 References

- 695 1. Cortini M, Avnet S, Baldini N (2017) Mesenchymal stroma: role
 696 in osteosarcoma progression. *Cancer Lett* 405:90–99
- 697 2. Kager L, Zoubek A, Dominkus M, Lang S, Bodmer N, Jundt
 698 G, Klingebiel T, Jürgens H, Gadner H, Bielack S, COSS Study
 699 Group (2010) Osteosarcoma in very young children. *Cancer Lett*
 700 116(22):5316–5324
- 701 3. Bielack S et al (2002) Prognostic factors in high-grade osteosarcoma
 702 of the extremities or trunk: an analysis of 1702 patients
 703 treated on neoadjuvant cooperative osteosarcoma study group
 704 protocols. *J Clin Oncol* 20(3):776–790

4. Alfranca A et al (2015) Bone microenvironment signals in osteosarcoma
 705 development. *Cell Mol Life Sci* 72(16):3097–3113
5. Lee SH, Shin MS, Park WS, Kim SY, Dong SM, Lee HK, Park
 706 JY, Oh RR, Jang JJ, Lee JY, Yoo NJ (1999) Immunohistochemical
 707 analysis of Fas ligand expression in normal human tissues. *J
 708 Pathol Microbiol Immunol* 107(11):1013–1019
6. Jia S, Worth LL, Kleinerman ES (1999) A nude mouse model of
 709 human osteosarcoma lung metastases for evaluating new therapeutic
 710 strategies. *Clin Exp Metastas* 17(6):501–506
7. Lafleur EA, Koshkina NV, Stewart J, Jia SF, Worth LL, Duan
 711 X, Kleinerman ES (2004) Increased Fas Expression Reduces the
 712 Metastatic Potential of Human Osteosarcoma Cells. *Clin Cancer
 713 Res* 10(23):8114–8119
8. Yang Y, Huang G, Zhou Z, Fewell JG, Kleinerman ES (2018)
 714 miR-20a regulates Fas expression in osteosarcoma cells by modulating
 715 Fas promoter activity and can be therapeutically targeted
 716 to inhibit lung metastases. *Mol Cancer Ther* 17(1):130–139
9. Xu WT, Bian ZY, Fan QM, Li G, Tang TT (2009) Human mesenchymal
 717 stem cells (hMSCs) target osteosarcoma and promote its growth and
 718 pulmonary metastasis. *Cancer Lett* 281(1):32–41
10. Lambert AW, Pattabiraman DR, Weinberg RA (2017) Emerging
 719 biological principles of metastasis. *Cell* 168(4):670–691
11. Fidler IJ (2003) The pathogenesis of cancer metastasis: the “seed and soil”
 720 hypothesis revisited. *Nat Rev Cancer* 3(6):453–458
12. Strilic B, Offermanns S (2017) Intravascular survival and extravasation
 721 of tumor cells. *Cancer Cell* 32(3):282–293
13. Chambers AF, Groom AC, MacDonald IC (2002) Dissemination and
 722 growth of cancer cells in metastatic sites. *Nat Rev Cancer* 2(8):563–572
14. Weis SM, Cheresh DA (2011) Tumor angiogenesis: molecular pathways
 723 and therapeutic targets. *Nat Med* 17(11):1359–1370
15. Carmeliet P (2000) Mechanisms of angiogenesis and arteriogenesis.
 724 *Nat Med* 6(4):389–395
16. Dvorak HF (2000) VPF/VEGF and the angiogenic response. *Semin Perinatol*
 725 24(1):75–78
17. Hempel N et al (2013) Acquisition of the metastatic phenotype is
 726 accompanied by H₂O₂-dependent activation of the p130Cas signaling
 727 complex. *Mol Cancer Res* 11(3):303–312
18. Almalki SG, Agrawal DK (2016) Effects of matrix metalloproteinases
 728 on the fate of mesenchymal stem cells. *Stem Cell Res Ther* 7(1):1–12
19. Bolontrade MF et al (2012) A specific subpopulation of mesenchymal
 729 stromal cell carriers overrides melanoma resistance to an oncolytic
 730 adenovirus. *Stem Cells Dev* 21(14):2689–2702
20. Passaniti A et al (1992) A simple, quantitative method for assessing
 731 angiogenesis and antiangiogenic agents using reconstituted basement
 732 membrane, heparin, and fibroblast growth factor. *Lab Invest* 67(4):519–528
21. Morales-Arias J et al (2007) Expression of granulocyte-colony-stimulating
 733 factor and its receptor in human Ewing sarcoma cells and patient tumor
 734 specimens: potential consequences of granulocyte-colony-stimulating
 735 factor administration. *Cancer* 110(7):1568–1577
22. Weidner N, Semple JP, Welch WR, Folkman J (1991) Tumor angiogenesis
 736 and metastasis—correlation in invasive breast carcinoma. *N Engl J Med*
 737 324(1):1–8
23. Weidner N et al (1992) Tumor angiogenesis: a new significant and
 738 independent prognostic indicator in early-stage breast carcinoma. *Natl
 739 Cancer Inst USA* 84(24):1875–1887
24. Bolontrade MF et al (1998) Angiogenesis is an early event in the
 740 development of chemically induced skin tumors. *Carcinogenesis* 19(12):
 741 2107–2113
25. Vitale DL, Spinelli FM, Del Dago D, Icardi A, Demarchi G, Caon I,
 742 García M, Bolontrade MF, Passi A, Cristina C, Alaniz L (2018) Co-
 743 treatment of tumor cells with hyaluronan plus doxorubicin
 744 745 746 747 748 749 750 751 752 753 754 755 756 757 758 759 760 761 762 763 764 765 766 767 768 769 770

- 771 affects endothelial cell behavior independently of VEGF expres-
772 sion. *Oncotarget* 9(93):36585
- 773 26. Calvo N et al (2019) PTHrP treatment of colon cancer cells pro-
774 motes tumor associated-angiogenesis by the effect of VEGF. *Mol*
775 *Cell Endocrinol* 483:50–63
- 776 27. Folkman J (2006) Angiogenesis. *Annu Rev Med* 57:1–18
- 777 28. Garcia MG et al (2005) Inhibition of NF-kappaB activity by BAY
778 11–7082 increases apoptosis in multidrug resistant leukemic
779 T-cell lines. *Leuk Res* 29(12):1425–1434
- 780 29. Barreiro Arcos ML et al (2013) Induction of apoptosis in
781 T lymphoma cells by long-term treatment with thyroxine
782 involves PKCzeta nitration by nitric oxide synthase. *Apoptosis*
783 18(11):1376–1390
- 784 30. Angulski AB, Capriglione LG, Batista M, Marcon BH, Senega-
785 glia AC, Stimamiglio MA, Correa A (2017) The protein content
786 of extracellular vesicles derived from expanded human umbilical
787 cord blood-derived CD133+ and human bone marrow-derived
788 mesenchymal stem cells partially explains why both sources
789 are advantageous for regenerative medicine. *Stem Cell Rev Rep*
790 13(2):244–257
- 791 31. Cox J, Mann M (2008) MaxQuant enables high peptide iden-
792 tification rates, individualized ppb-range mass accuracies
793 and proteome-wide protein quantification. *Nat Biotechnol*
794 26(12):1367–1372
- 795 32. Heldin CH, Westermark B (1999) Mechanism of action and
796 in vivo role of platelet-derived growth factor. *Physiol Rev*
797 79(4):1283–1316
- 798 33. Byrne AM, Bouchier-Hayes DJ, Harmey JH (2005) Angiogenic
799 and cell survival functions of vascular endothelial growth factor
800 (VEGF). *J Cell Mol Med* 9(4):777–794
- 801 34. Menges CW, Altomare DA, Testa JR (2009) FAS-Associated Factor
802 1 (FAF1): diverse functions and implications for oncogenesis. *Cell*
803 *Cycle* 8(16):2528–2534
- 804 35. Guerra B, Boldyreff B, Issinger OG (2001) FAS-associated factor
805 1 interacts with protein kinase CK2 in vivo upon apoptosis induc-
806 tion. *Int J Oncol* 19(6):1117–1126
- 807 36. Álvarez MV, Gutiérrez LM, Auzmendi J, Correa A, Lazarowski
808 A, Bolontrade MF (2020) Acquisition of stem associated-features
809 on metastatic osteosarcoma cells and their functional effects on
810 mesenchymal stem cells. *Biochim Biophys Acta* 1864(4):129522
- 811 37. Hanahan D, Coussens LM (2012) Accessories to the crime: func-
812 tions of cells recruited to the tumor microenvironment. *Cancer*
813 *Cell* 21(3):309–322
- 814 38. Mohan V, Das A, Sagi I (2020) Emerging roles of ECM remodel-
815 ing processes in cancer. *Semin Cancer Biol* 62:192–200
- 816 39. Aird WC (2007) Phenotypic heterogeneity of the endothelium: I.
817 Structure, function, and mechanisms. *Circ Res* 100(2):158–173
- 818 40. Ades EW et al (1992) HMEC-1: establishment of an immortal-
819 ized human microvascular endothelial cell line. *J Invest Dermatol*
820 99(6):683–690
- 821 41. Carter NM, Ali S, Kirby JA (2003) Endothelial inflammation:
822 the role of differential expression of N-deacetylase/N-sulphotrans-
823 ferase enzymes in alteration of the immunological properties of
824 heparan sulphate. *J Cell Sci* 116(Pt 17):3591–3600
- 825 42. Langley RR et al (2003) Tissue-specific microvascular endothelial
826 cell lines from H-2K(b)-tsA58 mice for studies of angiogenesis
827 and metastasis. *Cancer Res* 63(11):2971–2976
- 828 43. Ghosh S et al (2007) Use of multicellular tumor spheroids to dis-
829 sect endothelial cell-tumor cell interactions: a role for T-cadherin
830 in tumor angiogenesis. *FEBS Lett* 581(23):4523–4528
- 831 44. Harmey JH, Bouchier-Hayes D (2002) Vascular endothelial
832 growth factor (VEGF), a survival factor for tumour cells: impli-
833 cations for anti-angiogenic therapy. *BioEssays* 24(3):280–283
- 834 45. Chavakis E, Dimmeler S (2002) Regulation of endothelial cell
835 survival and apoptosis during angiogenesis. *Arterioscler Thromb*
836 *Vasc Biol* 22(6):887–893
46. Jia SF, Guan H, Duan X, Kleinerman ES (2008) VEGF165 is
837 necessary to the metastatic potential of Fas⁻ osteosarcoma cells
838 but will not rescue the Fas⁺ cells. *J Exp Ther Oncol* 7(2):89–97
839
47. Pidgeon GP, Barr MP, Harmey JH, Foley DA, Bouchier-Hayes DJ
840 (2001) Vascular endothelial growth factor (VEGF) upregulates
841 BCL-2 and inhibits apoptosis in human and murine mammary
842 adenocarcinoma cells. *Br J Cancer* 85(2):273–278
843
48. Zachary I, Glikli G (2001) Signaling transduction mechanisms
844 mediating biological actions of the vascular endothelial growth
845 factor family. *Cardiovasc Res* 49(3):568–581
846
49. Chen XL et al (2012) VEGF-induced vascular permeability is
847 mediated by FAK. *Dev Cell* 22(1):146–157
848
50. Hoang BH et al (2004) VEGF expression in osteosarcoma cor-
849 relates with vascular permeability by dynamic MRI. *Clin Orthop*
850 *Relat Res* 426:32–38
851
51. Weis SM, Cheresch DA (2005) Pathophysiological consequences of
852 VEGF-induced vascular permeability. *Nature* 437(7058):497–504
853
52. Daft PG, Yang Y, Napierala D, Zayzafoon M (2015) The growth
854 and aggressive behavior of human osteosarcoma is regulated by a
855 CaMKII-controlled autocrine VEGF signaling mechanism. *PLoS*
856 *ONE* 10(4):e0121568
857
53. Wang L, Zhang W, Ding Y, Xiu B, Li P, Dong Y, Zhu Q, Liang
858 A (2015) Up-regulation of VEGF and its receptor in refractory
859 leukemia cells. *Int J Clin Exp Pathol* 8(5):5282–5890
860
54. Papadopoulos N, Lennartsson J (2018) The PDGF/PDGFR path-
861 way as a drug target. *Mol Aspects Med* 62:75–88
862
55. Peng F et al (2008) Platelet-derived growth factor protects neurons
863 against gp120-mediated toxicity. *J Neurovirol* 14(1):62–72
864
56. Yilmaz A et al (2003) p38 MAPK inhibition is critically involved
865 in VEGFR-2-mediated endothelial cell survival. *Biochem Biophys*
866 *Res Commun* 306(3):730–736
867
57. Eppihimer MJ et al (1998) Differential expression of platelet-
868 endothelial cell adhesion molecule-1 (PECAM-1) in murine tis-
869 sues. *Microcirculation* 5(2–3):179–188
870
58. Mammoto A, Mammoto T (2019) Vascular niche in lung alveolar
871 development, homeostasis, and regeneration. *Front Bioeng Bio-*
872 *technol* 7:318
873
59. Pezzella F et al (1997) Non-small-cell lung carcinoma tumor
874 growth without morphological evidence of neo-angiogenesis. *Am*
875 *J Pathol* 151(5):1417–1423
876
60. Sardari Nia P et al (2007) Distinct angiogenic and non-angiogenic
877 growth patterns of lung metastases from renal cell carcinoma.
878 *Histopathology* 51(3):354–361
879
61. Matei D et al (2007) PDGF BB induces VEGF secretion in ovarian
880 cancer. *Cancer Biol Ther* 6(12):1951–1959
881
62. Langley RR et al (2004) Activation of the platelet-derived growth
882 factor-receptor enhances survival of murine bone endothelial
883 cells. *Cancer Res* 64(11):3727–3730
884
63. Lee C et al (2010) Reduced levels of IGF-I mediate differential
885 protection of normal and cancer cells in response to fasting and
886 improve chemotherapeutic index. *Cancer Res* 70(4):1564–1572
887
64. Knowles J, Loizidou M, Taylor I (2005) Endothelin-1 and angio-
888 genesis in cancer. *Curr Vasc Pharmacol* 3(4):309–314
889
65. Kim SW et al (2014) Role of the endothelin axis in astrocyte- and
890 endothelial cell-mediated chemoprotection of cancer cells. *Neuro*
891 *Oncol* 16(12):1585–1598
892
66. Xie F et al (2017) FAF1 phosphorylation by AKT accumulates
893 TGF- β type II receptor and drives breast cancer metastasis. *Nat*
894 *Commun* 8:15021
895
67. Zhang L, Zhou F, van Laar T, Zhang J, van Dam H, Ten Dijke
896 P (2011) Fas-associated factor 1 antagonizes Wnt signaling by
897 promoting β -catenin degradation. *Mol Biol Cell* 22(9):1617–1624
898
68. LaBiche RA, Tresslert RJ, Nicolson GL (1993) Selection for
899 enhanced adhesion to microvessel endothelial cells or resist-
900 ance to interferon- γ modulates the metastatic potential of murine
901

- 902 RAW117 large-cell lymphoma cells. *Clin Exp Metastasis* 11(6):472–481
- 903
- 904 69. Hansen AG, Arnold SA, Jiang M, Palmer TD, Ketova T, Merkel A, Pickup M, Samaras S, Shyr Y, Moses HL, Hayward SW (2014) ALCAM/CD166 is a TGF- β -responsive marker and functional regulator of prostate cancer metastasis to bone. *Cancer Res* 74(5):1404–1415
- 905
- 906
- 907
- 908 70. Soto MS et al (2014) Functional role of endothelial adhesion molecules in the early stages of brain metastasis. *Neuro Oncol* 16(4):540–551
- 909
- 910
- 911
- 912 71. Degen WG et al (1998) MEMD, a new cell adhesion molecule in metastasizing human melanoma cell lines, is identical to ALCAM (activated leukocyte cell adhesion molecule). *Am J Pathol* 152(3):805–813
- 913
- 914
- 915 72. Guerra B, Boldyreff B, Issinger OG (2001) FAS-associated factor 1 interacts with protein kinase CK2 in vivo upon apoptosis induction. *Int J Oncol* 19(6):1117–1126
- 916
- 917
- 918 73. Qin L, Guo J, Zheng Q, Zhang H (2016) BAG2 structure, function and involvement in disease. *Cell Mol Biol Lett* 21(1):1–11
- 919
- 920
- 921 74. Yunoki T, Tabuchi Y, Kondo T, Ishii Y, Hayashi A (2017) Overexpression of the anti-apoptotic protein BAG3 in human choroidal melanoma: a case report. *Oncology Lett* 13(6):4169–4172
- 922
- 923
- 924 75. Bruchmann A, Roller C, Walther TV, Schäfer G, Lehmusvaara S, Visakorpi T, Klocker H, Cato AC, Maddalo D (2013) Bcl-2 associated athanogene 5 (Bag5) is overexpressed in prostate cancer and inhibits ER-stress induced apoptosis. *BMC Cancer* 13(1):1–11
- 925
- 926
- 927
- 928 76. Krenciute G, Liu S, Yucer N, Shi Y, Ortiz P, Liu Q, Kim BJ, Odejimi AO, Leng M, Qin J, Wang Y (2013) Nuclear BAG6-UBL4A-GET4 complex mediates DNA damage signaling and cell death. *J Biol Chem* 288(28):20547–20557
- 929
- 930
- 931 77. Pawlowski J, Kraft AS (2000) Bax-induced apoptotic cell death. *Proc Natl Acad Sci USA* 97(2):529–531
- 932
- 933 78. Jensen SA et al (2014) Bcl2L13 is a ceramide synthase inhibitor in glioblastoma. *Proc Natl Acad Sci USA* 111(15):5682–5687
- 934
- 935 79. Shao AW et al (2016) Bclaf1 is an important NF- κ B signaling transducer and C/EBP β regulator in DNA damage-induced senescence. *Cell Death Differ* 23(5):865–875
- 936
- 937 80. Bousquet G et al (2019) High expression of apoptosis protein (Api-5) in chemoresistant triple-negative breast cancers: an innovative target. *Oncotarget* 10(61):6577–6588
- 938
- 939 81. Sharma M (2013) Apoptosis-antagonizing transcription factor (AATF) gene silencing: role in induction of apoptosis and down-regulation of estrogen receptor in breast cancer cells. *Biotechnol Lett* 35(10):1561–1570
- 940
- 941 82. Bano D, Prehn JH (2018) Apoptosis-inducing factor (AIF) in physiology and disease: the tale of a repented natural born killer. *EBioMedicine* 30:29–37
- 942
- 943
- 944
- 945
- 946
- 947
- 948
- 949 **Publisher's Note** Springer Nature remains neutral with regard to jurisdictional claims in published maps and institutional affiliations.
- 950
- 951

Journal:	10495
Article:	1677

Author Query Form

Please ensure you fill out your response to the queries raised below and return this form along with your corrections

Dear Author

During the process of typesetting your article, the following queries have arisen. Please check your typeset proof carefully against the queries listed below and mark the necessary changes either directly on the proof/online grid or in the 'Author's response' area provided below

Query	Details Required	Author's Response
AQ1	Please confirm if the author names are presented accurately and in the correct sequence (given name, middle name/initial, family name). Author 1 Given name: [Matías Valenzuela] Last name [Alvarez]. Author 2 Given name: [María Jose] Last name [Cantero]. Also, kindly confirm the details in the metadata are correct.	
AQ2	Please check and confirm that the authors and their respective affiliations have been correctly identified and amend if necessary.	
AQ3	References [72-83] were provided in the reference list; however, these were not mentioned or cited in the manuscript. As a rule, if a citation is present in the text, then it should be present in the list. Please provide the location of where to insert the reference citation in the main body text. Kindly ensure that all references are cited in ascending numerical order.	
AQ4	AUTHOR: As References 82. and 83. are same, we have deleted the duplicate reference and renumbered accordingly. Please check and confirm.	

Author Proof